Available online at www.sciencedirect.com
ScienceDirect
Dyes and Pigments 75 (2007) 263–272
DYES and PIGMENTS
www.elsevier.com/locate/dyepig

Preparation and characterization of activated carbon from oil palm wood and its evaluation on Methylene blue adsorption

A.L. Ahmad [a,*], M.M. Loh [a], J.A. Aziz [b]

[a] School of Chemical Engineering, Engineering Campus, Universiti Sains Malaysia, Seri Ampangan, 14300 Nibong Tebal, S.P.S., Pulau Pinang, Malaysia
[b] School of Mechanical Engineering, Engineering Campus, Universiti Sains Malaysia, Seri Ampangan, 14300 Nibong Tebal, S.P.S., Pulau Pinang, Malaysia

Received 24 October 2005; received in revised form 12 February 2006; accepted 20 May 2006
Available online 18 July 2006

Abstract

Activated carbons were prepared from the biomass of oil palm wood (OPW) via two stages, pyrolysis and physical activation, using an environmentally friendly pyrolysis pilot plant, and an activation pilot plant was studied. The latter uses the outlet flue gases from limestone calcination process as activating agents. Experimental results showed that pyrolysis and activation conditions leading to various final average temperatures had significant effect on the properties of activated carbons prepared. Suitable pyrolysis operating conditions of 7 $m^3 h^{-1}$ airflow rate for 4 h until final average pyrolysis temperature 390 °C and activation conditions of 7.45 kg limestone calcined with airflow rate 202.4 ml s^{-1} for 3.5 h until final average activation temperature of 806 °C produced an activated carbon yield of 13.7%, 68.3% fixed carbon, 16.9% volatile matters, 4.3% ash, and 10.6% moisture, and 1084 $m^2 g^{-1}$ BET surface area, and a micropore surface area of 931.6 $m^2 g^{-1}$ was obtained. Methylene blue adsorption was tested and 90.9 mg g^{-1} maximum adsorption capacity was found. The high micropore fraction, N_2 adsorption isotherm and SEM showed that these activated carbons possessed intricate pore network comprising micropores and narrow mesopores. FTIR characterization indicated that pyrolysis and activation temperatures affected the surface functional groups and maximum Methylene blue adsorption was dependent on BET surface area.

Keywords: Activated carbon; Methylene blue; Pyrolysis; Activation; BET Surface areas; Langmuir isotherm

1. Introduction

Activated carbons (AC) are carbonaceous materials that have highly developed porosity and internal surface area of more than 400 $m^2 g^{-1}$ [1]. They are widely used as adsorbents in wastewater and gas treatments as well as in catalysis. The increasing usage and competitiveness of activated carbon prices, has prompted the usage of agricultural by-products such as fruit stones [2], coconut shell [3] and rice straw [5] as raw materials to prepare AC. These solid wastes are not only cheap and easily available but are considered as wastes that contribute to disposal problems.

In Malaysia, oil palm trunk is one of the main agricultural waste generated by the flourishing palm oil industries. In the year 2000, about 7.02 million oil palm trunks were generated and this waste was left to rot, burnt off in stacks or used as mulch [5]. Realizing the scale of this waste, several studies were initiated to convert oil palm wood (OPW) to value added products. Hoi and Akmar [7] and Lim and Lim [8] tried pyrolyzing oil palm wood to charcoal. However, due to the friable nature of the wood, low calorific value was obtained and there were difficulties in controlling the conversion efficiency as well as pyrolysis rate, hence, suggesting that oil palm wood charcoal was unsuitable to be used as charcoal fuel. The use of oil palm wood as raw material for activated carbon was

* Corresponding author. Tel.: +604 5937788/6418; fax: +604 5941013.
E-mail address: chlatif@eng.usm.my (A.L. Ahmad).

0143-7208/$ - see front matter © 2006 Elsevier Ltd. All rights reserved.
doi:10.1016/j.dyepig.2006.05.034

Nomenclature

$Y_{charcoal}$	Charcoal yield (%)
Y_{lp}	Liquid by-product yield (%)
$Y_{activated\ carbon}$	Overall activated carbon yield (%)
W_w	Mass of wood (kg)
W_c	Mass of charcoal (kg)
W_f	Mass of fuel (kg)
W_{AC}	Mass of activated carbon (kg)
Q_o	Langmuir maximum monolayer adsorption capacity (mg g^{-1})
C_o	Initial dye concentration (mg L^{-1})
C_e	Equilibrium dye concentration (mg L^{-1})
q_e	Amount of dye adsorbed at equilibrium (mg)
b	Langmuir constant (L mg^{-1})
P/P_0	Relative pressure (−)

highlighted by Hussein et al. [9], and they showed that the combination of chemical (impregnation with zinc chloride) and physical activation method could be used to produce activated carbon with fairly high surface area.

In general, activated carbons are produced by pyrolyzing raw materials to form charcoal and subsequently activating the charcoal using mild oxidizing gases such as carbon dioxide, steam and flue gases at high temperatures ranging from 500 °C to 1000 °C. Investigations have shown that different raw materials would produce different quality of activated carbons [10].

The objective of this study was to prepare relatively well-developed porosity activated carbons from oil palm wood in a pilot plant via physical methods and to study the various conditions as well as parameters that are involved during the process. The oil palm wood activated carbon (OPWAC) was fully characterized. Its composition, morphological changes and surface functional groups were analyzed. Its performance for liquid adsorption capacity was evaluated using Methylene blue dye.

2. Materials and method

2.1. Raw oil palm wood

Oil palm woods were obtained from our Engineering campus in Nibong Tebal, Penang, debarked and cut into blocks with average dimensions of 5 cm × 5 cm × 30 cm. Then, the blocks were air dried under natural conditions for about two months. A thermogravimetric analyzer (Perkin Elmer/TGA7) was used to carry out the proximate analysis, which was expressed in terms of fixed carbon, volatile matters, ash and moisture content. The characteristics of the raw wood are shown in Table 1.

2.2. Pyrolysis process

The pyrolysis pilot plant as shown in Fig. 1, consists of an air intake system, a pilot kiln, pilot pollution prevention chamber, scrubber, cross flow cooling tower, constant head tank system and wastewater reservoir tank. The pilot kiln (made from cast iron and coated with ceramic) is divided into four chambers: air distributor and ash collection chamber, combustion chamber, economizer chamber and pyrolysis chamber. The pyrolysis chamber has the dimensions of 50 cm height, 45 cm lower diameter and 30 cm upper diameter. Bed temperatures of the pyrolysis chamber are measured using 15 Type-K thermocouples connected to Digi Sense Scanning Thermometer (Cole Parmer Model: 92000-05).

Table 1
Raw oil palm wood characteristics

Sample	Fixed carbon (wt%)	Volatile matters (wt%)	Ash (wt%)	Moisture (wt%)	Overall average density (kg m^{-3})
OPW[a]	9.63	76.58	1.95	11.83	215

[a] OPW represents oil palm wood.

Per batch, approximately 3.9 kg of wood was placed in the pyrolysis pilot kiln. The combustion chamber was charged with approximately 3 kg of waste rubber wood as fuel. From preliminary studies regarding the effect of airflow rate on final pyrolysis temperatures, the pyrolysis process was carried out using the suitable airflow rate of 7 $m^3\ h^{-1}$ that provided steady state fuel combustion and steady state pyrolysis. The pyrolysis period was varied from 3 to 6 h in this work to achieve final average pyrolysis temperature of 350–420 °C. Once the process was completed, the kiln was cooled for 12 h to reach ambient temperature via natural convection.

The charcoal, liquid by-product and ash were weighed. Charcoal yields, $Y_{charcoal}(\%)$, and liquid by-product yield, $Y_{liquid\ by\text{-}product}(\%)$, were calculated as follows:

$$Y_{charcoal}(\%) = (W_c/W_w) \times 100 \quad (1)$$

$$Y_{liquid\ by\text{-}product}(\%) = \left(W_{lp} \times 100\right)/\left(W_w + W_f\right) \quad (2)$$

where W_w is the mass of wood used as feed for pyrolysis, W_c is the mass of charcoal, W_{lp} is the mass of liquid by-product and W_f is the mass of fuel.

2.3. Activation process

The activation pilot plant as shown in Fig. 2, consists of a combustion system of liquefied petroleum gases (LPG), activation kiln, spiral jacketed baffled cooler and an air intake–outlet system. The activation kiln is made from mild steel and insulated with castable cement. It has the dimension of 166.5 cm height and 59 cm diameter. Temperature monitoring was carried out using 20 Type-K thermocouples connected to Digi Sense Scanning Thermometer (Cole Parmer Model: 92000-05).

Charcoal produced in the pyrolysis pilot plant was subsequently used as raw material for the activation process, which

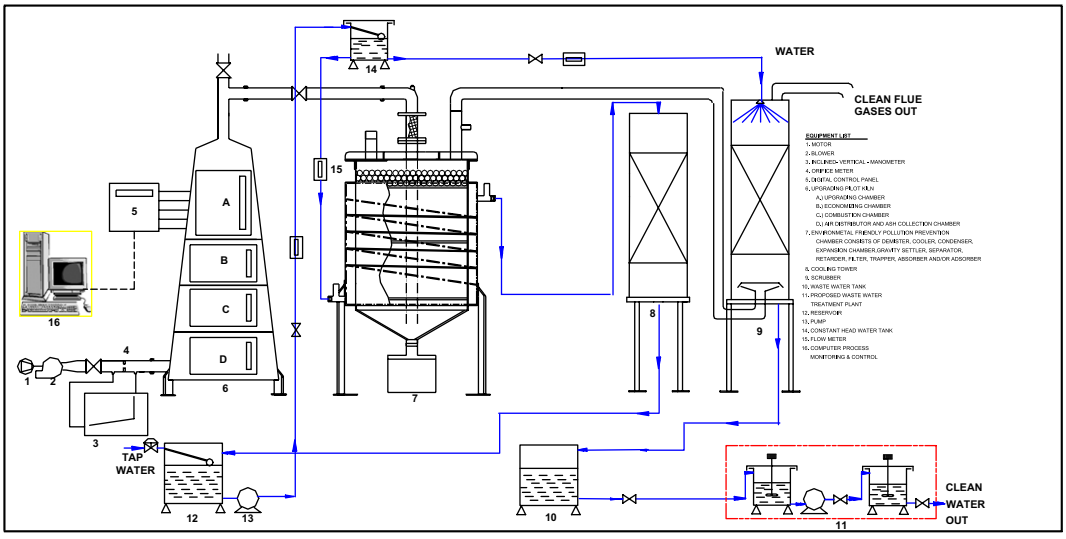

Fig. 1. Schematic diagram of the pyrolysis pilot plant.

was carried out in an activation pilot plant. The charcoal was cut into 1 cm × 1 cm × 1 cm cubes. Charcoal cubes of 8 g were filled into an activation cylinder and then placed into the activation kiln. In addition, 7.45 kg of limestone (corresponding to five layers) was also loaded into the activation kiln. Preliminary studies have shown that calcination of five layers of limestone provided a high temperature profile and was sufficient to avoid the activation cylinder from direct contact with the flame coming from the LPG combustion system. Limestone was fired using temperatures above limestone decomposition point (825 °C) at airflow rate 202.4 ml s^{-1} and the following reactions occurred:

$$CaCO_3(\text{limestone}) + \text{heat} \rightarrow CaO(\text{quick lime}) + CO_2 \quad (3)$$

$$\text{LPG} + \text{air} \rightarrow CO_2 + H_2O + N_2 \quad (4)$$

Carbon dioxide (CO_2) and steam (H_2O) released were used as mild oxidizing gases to activate the charcoal. By varying activation periods (1–3.5 h), the temperature of activation gases was raised from room temperature to certain final average activation temperatures (519–806 °C). After activation, the kiln was cooled to ambient temperature before weighing the amount of OPWAC produced. Overall activated carbon yield, $Y_{\text{activated carbon}}(\%)$, was calculated based on the initial weight of wood used as raw material for pyrolysis and activation. The equation applied is as follows:

$$Y_{\text{activated carbon}}(\%) = (W_{\text{ac}}/W_{\text{w}}) \times 100 \quad (5)$$

where W_{ac} is the mass of activated carbon after activation and W_{w} is the mass of wood used as feed for pyrolysis. Prior to characterization, the activated carbon was soaked in 0.05 M hydrochloric acid for 1 h to remove alkali and alkaline earth, washed with deionized water until free of measurable chloride (pH 6–7) and then oven dried at 110 °C for 6 h to remove moisture [4,5]. Once dried, the activated carbon cubes were crushed using a mortar and pestle and sieved to sizes ranging

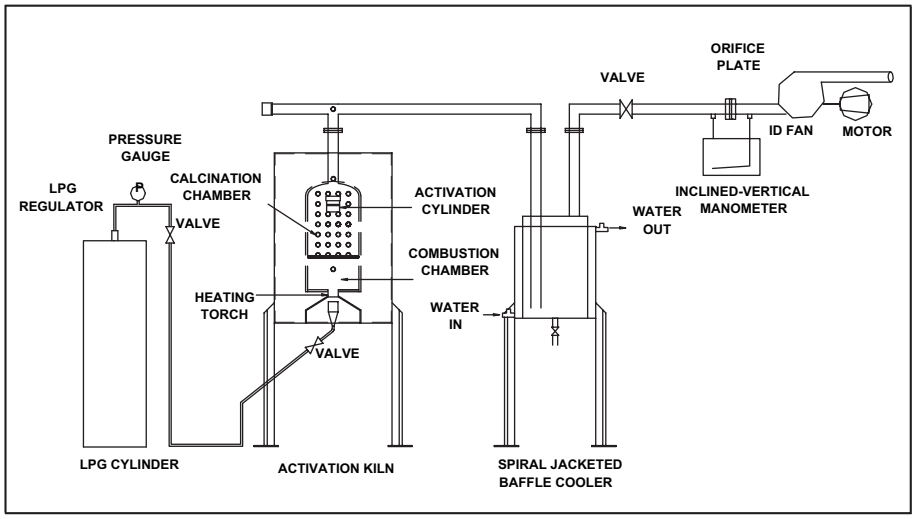

Fig. 2. Schematic diagram of activation pilot plant.

from 0.71 to 1 mm and 1 to 2 mm to be used for analysis and adsorption experiments.

2.4. Textural and chemical characterization

Adsorption characterization for activated carbon obtained at different pyrolysis periods was determined via nitrogen adsorption at −196 °C using Autosorb-1 Quantachrome Automated Gas Sorption System. The Brunauer-Emmett-Teller (BET) total surface area and t-method micropore surface area were calculated from the adsorption isotherms using the BET equation and de Boer's 't-method', respectively [11]. Micropore fraction (percent ratio of micropore surface area to the BET total surface area) was also tabulated to study the pore development at the respective pyrolysis period [2]. A scanning microscope (Model Leo Supra) equipped with an energy dispersive X-ray microanalysis (Oxford INCA) was used to determine the surface textural characteristics and elemental composition of AC. The surface organic structures were studied using Fourier transformed infra-red spectroscopy (Perkin Elmer Series II IR) over the wavelength range of 4000–400 cm^{-1}.

2.5. Methylene blue adsorption

Due to its strong adsorption onto solids, Methylene blue dye serves as a model compound for adsorption of organic contaminant from aqueous solutions [12–14]. For batch adsorption studies, 0.05 g activated carbon was added to a series of Erlenmeyer flasks filled with 50 ml Methylene blue concentrations ranging from 10 to 250 mg L^{-1}, sealed with parafilm and then shaken at 125 rpm under 30 °C in an orbital shaker incubator until equilibrium was reached. The sample solution was then removed using a syringe and analyzed with a spectrophotometer at a wavelength of 660 nm. The amount of dye adsorbed, q_e was calculated using Eq. (6) and fitted to the Langmuir equilibrium model in Eq. (7):

$$q_e = V(C_o - C_e)/M \quad (6)$$

$$C_e/q_e = (1/Q_o b) + (C_e/Q_o) \quad (7)$$

where q_e is the amount of dye adsorbed at equilibrium, C_e, the equilibrium dye concentration, C_o, the initial dye concentration, Q_o, the Langmuir maximum monolayer adsorption capacity and b, the Langmuir constant [13].

3. Results and discussion

3.1. Pyrolysis

In this work, final pyrolysis temperature was found to be dependent on the pyrolysis period. Table 2 shows the final average pyrolysis temperature, charcoal yield, product/fuel ratio and proximate analysis at various pyrolysis periods.

Final pyrolysis temperature increased non-linearly with increasing pyrolysis period due to endothermic and exothermic chemical reactions throughout the process [15–17]. Charcoal yield seemed to decrease from 30.5% to 21.6% as pyrolysis period was prolonged. The decrease was due to devolatilization and thermal degradation of extractives as well as high-molecular-weight hydrocarbons [18]. In addition, as the pyrolysis period increased from 3 to 6 h, the volatile matters in charcoal decreased from 47.34% to 14.77% while fixed carbon increased. Ash content increases from 1.95% (in oil palm wood) to 6.30% after a pyrolysis period of 6 h. This was expected as increased devolatilization during pyrolysis resulted in charcoal containing predominantly carbon [2,18]. Furthermore, moisture content also decreased from 7.22% to 5.34%. Higher temperatures obtained by prolonging pyrolysis period caused the carboxylic and phenolic structures in charcoal to decompose. Hence, CO_2 which forces bound water to be expelled from the pores was produced [19].

With reference to the published data by other authors [15,20–22], airflow rate of 7 $m^3 h^{-1}$ and 4 h of pyrolysis period were chosen as the suitable operating conditions for the pyrolysis process, hence, producing 28.5% charcoal yield and 0.2 product/fuel ratio and charcoal quality of 63.23% fixed carbon, 25.15% volatile matters, 6.19% ash and 5.42% moisture. These conditions utilized reasonable fuel consumption and provided high amounts of charcoal to be used as raw material in the subsequent activation stage. Furthermore, they were also observed as stable operating conditions for fuel combustion and stable conditions for pyrolysis owing to the

Table 2
Final average pyrolysis temperature, charcoal yield, product/fuel ratio and proximate analysis for oil palm wood, charcoal obtained using airflow rate of 7 $m^3 h^{-1}$ at various pyrolysis periods

Sample	Pyrolysis period (h)	Final average pyrolysis temperature (°C)	Yield, $Y_{charcoal}$ (%)	Product/fuel ratio	Fixed carbon (wt%)	Volatile matters (wt%)	Ash (wt%)	Moisture (wt%)
OPW	–	–	–	–	9.63	76.58	1.95	11.83
OPWC3	3	350	30.5	0.2	39.25	47.34	6.20	7.22
OPWC4	4	390	28.5	0.2	63.23	25.15	6.19	5.42
OPWC5	5	415	23.9	0.16	68.41	19.96	6.24	5.38
OPWC6	6	420	21.6	0.09	73.59	14.77	6.30	5.34
Published data [15,20,21,22]	–	400–500	20–30	–	>60	15–30	2–5	5–15

Note: OPW represents oil palm wood.
OPWC represents oil palm wood charcoal.

sensitivity of oil palm wood to undergo incomplete combustion once exposed to excess amounts of oxygen.

3.2. Activation

Similar to prior pyrolysis process, preliminary studies using the activation plant have shown that the final average activation temperature was dependent on activation period. As shown in Table 3, activation temperatures seemed to be increasing as activation periods increase. However, the temperature differences decreased as activation periods were increased due to the narrowing temperature gradient (smaller driving force) between the inside kiln temperatures and flame temperatures.

3.2.1. Yield of activated carbon

In most processes, relatively high yield of activated carbon is required. Table 3 shows the final average activation temperature, overall activated carbon yield and proximate analysis obtained by varying activation periods. The activated carbon yield was seen to decrease from 21.6% to 13.4% as activation period increased from 1 to 3.5 h. Final average activation temperatures increased from 519 °C to 806 °C as activation period increased. During these temperatures, there was a combination of continual devolatilization of volatile matters and carbon–CO_2 [23] as well as carbon–H_2O reaction [24] due to the presence of CO_2 and H_2O in the activation gases. The decrease was more distinct at higher periods and temperatures due to increasing rate of reaction between carbon and CO_2, which resulted in the development of internal surface area and porosity [23]. Furthermore, during pyrolysis, some of the pores might have been blocked by deposition of carbonaceous tar materials during the cooling period after pyrolysis [25]. Hence, at lower temperatures, steam was more likely to have had first eliminated these materials [26] before proceeding with the carbon–H_2O reactions, which increases rapidly as activation temperature increases [24]. The range of yield obtained, 25–12%, was similar to that reported in other works [5,23].

Table 3 also shows that as the activation period increased from 1 to 3.5 h, fixed carbon also increased from 56.5% to 68.3%, whereas volatile matters decreased from 47.3% to 14.8%. Steam had the ability to penetrate into the solid material and further helped in desorption, distillation and more efficient removal of the volatiles still remaining in the charcoal. It also helped in stabilizing the radicals obtained during thermal decomposition, hence increasing the removal of volatile matter [25]. Even though some fixed carbon content was lost during activation reactions, these reductions were marred by more volatile matter losses. Hence, the decrease was not reflected in the data collected [23]. Instead, an increasing fixed carbon trend was obtained. As for ash content, it ranged from 5.1% to 4.3% as activation period was increased. The difference in ash content was not distinct, as ash is not destroyed during pyrolysis activation [27]. However, the ash content in activated carbon was lower compared to charcoal due to acid washing [4]. No distinct trend could be seen for moisture content (ranged from 7.0% to 10.1%) as activation period was increased. This was due to the hydroscopic nature of activated carbon that absorbs moisture from the surrounding atmosphere and steam. Nevertheless, this range is comparable with other steam activated wood based activated carbon that have about 10% moisture content [28].

3.2.2. Porosity, surface area and average pore size

The adsorption capacity of activated carbons can be identified from their physical characteristics such as porosity, surface area and pore size. Fig. 3 shows the isotherms of nitrogen adsorption at −196 °C for charcoal and oil palm wood activated carbons prepared using different activation periods. The amount of N_2 adsorbed by charcoal slightly increases as relative pressure (P/P_0) increases to values higher than 0.99. However, this low adsorption volume indicated that after the pyrolysis stage, charcoal still contained very little amount of pores. Its microporous structure is yet to be fully developed.

After 1 h of activation, the isotherm began changing to Type I isotherm. A more pronounced increase in the volume of N_2 adsorbed for low P/P_0 and a weak increase at higher P/P_0 (almost horizontal plateau) indicated the dominant presence of micropores in the activated carbon [29]. The CO_2 in the activating gases mixture has a mean diameter of around 1.5 nm. Hence, CO_2 tends to develop narrower micropores in the activated carbon [30].

As the activation period was increased to 1.5 h (higher average activation temperature of 620 °C), Type II isotherm was detected. Here, the slope at low P/P_0 became steeper,

Table 3
Final average activation temperature, yield, and proximate analysis for activated carbon obtained using 7.45 kg limestone and gas flow rate of 202.4 ml s^{-1} at various activation periods

Sample	Activation period (h)	Final average activation temperature (°C)	Yield, $Y_{\text{activated carbon}}$ (%)	Fixed carbon (wt%)	Volatile matters (wt%)	Ash (wt%)	Moisture (wt%)
OPWAC1	1	519	21.6	56.5	29.2	5.1	9.2
OPWAC1.5	1.5	619	21.3	54.9	31.7	4.4	9.1
OPWAC2	2	675	18.7	63.3	25.0	4.7	7.0
OPWAC2.5	2.5	755	18.6	59.7	26.3	4.6	9.4
OPWAC3	3	798	15.5	61.1	24.7	4.1	10.1
OPWAC3.5	3.5	806	13.4	68.3	18.0	4.3	9.5
Other works [5,23]	–	500–900	25–12	>70	<20	<7	<10

Note: OPWAC represents oil palm wood activated carbon.

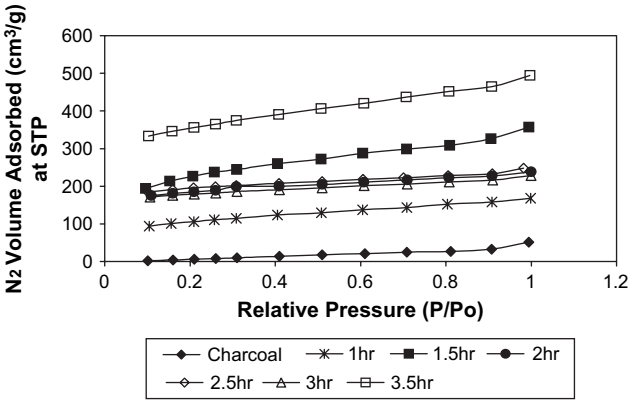

Fig. 3. Volume of N_2 adsorbed versus relative pressure for activated carbon prepared at various activation periods.

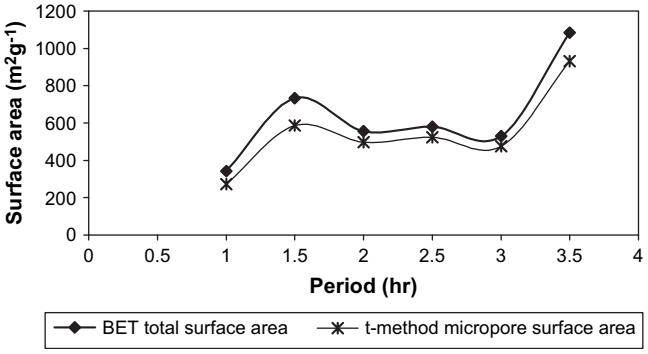

Fig. 4. Surface area versus activation period.

indicating that there was a great increase in micropores due to newly created micropores. Nevertheless, the increased steepness of the gradient and a more marked increase in quantity adsorbed at higher P/P_0 also suggested the presence of wider porosity, mainly supermicropores and mesopores. It was mentioned earlier that besides CO_2, the activating gases also contain H_2O that has a mean diameter of 2 nm. It has caused the development of supermicro and even mesopore in the carbon [30]. For the activation periods of 2, 2.5 and 3 h, the overall volume of N_2 adsorbed for all P/P_0 was much lower compared to the isotherm obtained at 1.5 h. The shape of the isotherms returned to that of the Type I isotherms representing microporous solids with relatively small external surface area. High temperatures had caused some narrowing of pore structures and the presence of intermediate melt caused the closures of some of the newly created pores during earlier activation periods [31]. For activation periods beyond 3 h, some of these melts were vaporized and there was continuous release of high-molecular-weight volatiles [30]. At 3.5 h, higher rate of carbon ''burn-off'' had increased the amounts of mesopores. Hence, drastically increasing the overall volume of N_2 adsorbed especially at high P/P_0.

In accordance with the IUPAC classification, all the samples (both charcoal and activated carbons) were generally said to possess isotherms belonging to a mix of Type I isotherms, which are associated with microporous solids, and Type II isotherms, which are associated with mesoporous structures. Hence, inferring that the activated carbons prepared from oil palm wood had a mixture of micropores and mesopores.

The effect of activation period on BET and micropore surface area is shown in Fig. 4. As activation period increased to 1.5 h, BET surface area increased from 194.7 $m^2\,g^{-1}$ in charcoal to 733.1 $m^2\,g^{-1}$ due to the evolution of volatiles remaining in the charcoal and creation of new pores due to carbon–CO_2 and carbon–H_2O reactions [23]. However, further increase in activation period from 1.5 h (619 °C) to 3 h (798 °C) caused BET surface area to decline to 529 $m^2\,g^{-1}$. This could be attributed to the formation of intermediate melt in the charcoal in addition to evolution of secondary volatiles, which softens the intermediate melt. Hence, softening causes closure of some of the newly created pores and eventually pore enlargement [30]. Nevertheless as the activation period was increased from 3 h (790 °C) to 3.5 h (806 °C), BET surface area increased again to about 1084 $m^2\,g^{-1}$. At 3.5 h (806 °C), the intermediate melts were vaporized and there was continual release of high-molecular-weight volatiles creating openings of additional pores, which lead to an increase in BET surface area [30]. The t-method micropore surface area curve showed a trend similar to that of the BET surface area curve.

Fig. 5 shows the plot of the micropore fraction versus activation period. It is observed that the micropore fraction increases to 90.3% as activation period increased to 2.5 h. However, the micropore fraction slightly decreased to 86.0% after 3.5 h. This drop was due to increasing carbon–CO_2 and carbon–H_2O reaction rates, which cause the burning of adjacent micropore walls (creating mesopores and macropores), mass losses due to exterior activation and particle shrinkage with less new micropore development [32].

The dominant effect of small and medium sized pores in activated carbon was also observed from Fig. 6. According to IUPAC classification, the widths of micropores are less than 2 nm (20 Å), that of mesopores between 2 nm (20 Å) and 50 nm (500 Å) and macropores are greater than 50 nm (500 Å). As charcoal was activated till 2.5 h, the average pore size decreased to 22.63 Å owing to the creation of more narrow micropores and blockage of pores by

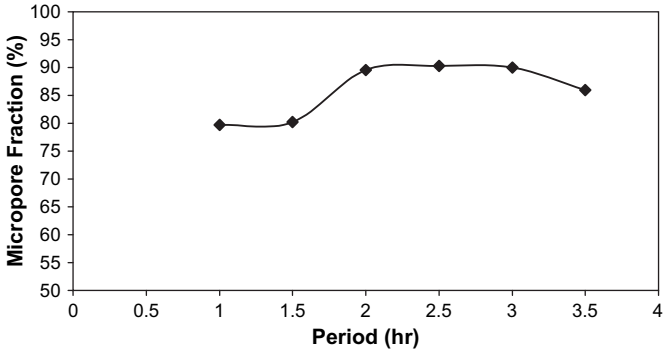

Fig. 5. Micropore fraction versus activation using 7.45 kg limestone and airflow rate of 202.4 ml s^{-1}.

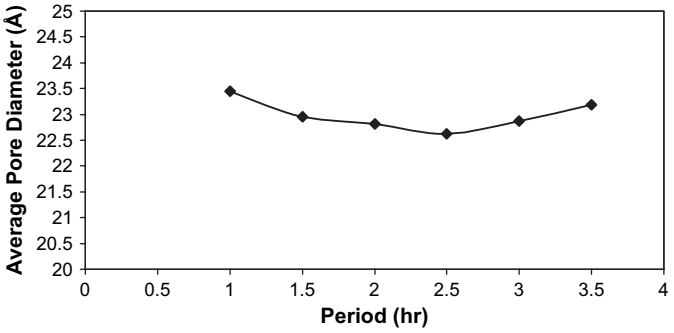

Fig. 6. Average pore diameter versus activation period using 7.45 kg limestone and gas flow rate of 202.4 ml s^{-1}.

intermediate melt. However, activation periods exceeding 2.5 h lead to an increased average pore size, implying bigger pore development due to severe carbon ''burn-off''. These observations agreed with the increasing and decreasing micropore fraction (%) mentioned earlier. Overall pore diameter width for oil palm wood activated carbon lay more to the range of micropore and narrow mesopore.

3.2.3. Scanning electron micrographs (SEM)

SEM studies the structural changes in wood anatomy during pyrolysis and activation. Fig. 7 shows the 500× magnification for (a) oil palm wood, (b) charcoal and (c) activated carbon. The wood surface has a relatively smooth solid structure mainly void of pores but with occasional crevices. Similar to other SEM works [33], the wood surface was also covered with many globular silica bodies that contain sharp, conical agglomerations. It was also noted that there was a thickening of the basal cell forming a hat-like brim, and depressions into the wood surface to accommodate the silica body. However, when the wood was subjected to pyrolysis, there was rupturing of parenchymatic ground tissues. The solid surface was transformed to uneven textures and layers. The presence of small pores on the surface showed that charcoal was starting to develop a rudimentary pore network. Moreover, the silica globules seemed to be more exposed due to the leveling off or shrinkage of the thick basal cell brim.

From Fig. 7(c), it can be deduced that activation with carbon dioxide and steam increases attacks on the solid surface with the formation of various sizes of pits, which make up distinct micropores, mesopores and macropores. This, thereby, increases BET surface area from 194.7 $m^2 g^{-1}$ in charcoal to 1084.0 $m^2 g^{-1}$ in activated carbon.

3.2.4. Fourier transformed infra-red (FTIR) spectroscopy

Besides porosity, adsorption behavior of activated carbon is also influenced by the chemical reactivity of the surface especially in the form of chemisorbed oxygen in various forms of functional groups. These surface oxides have acidic as well as basic properties [34]. FTIR was carried out on samples of oil palm wood (OPW), oil palm wood charcoal (OPWC), Norit GAC 1240 (commercial activated carbon) and oil palm wood activated carbon (OPWAC), which had undergone an activation period of 3.5 h. Fig. 8 shows that the functional groups

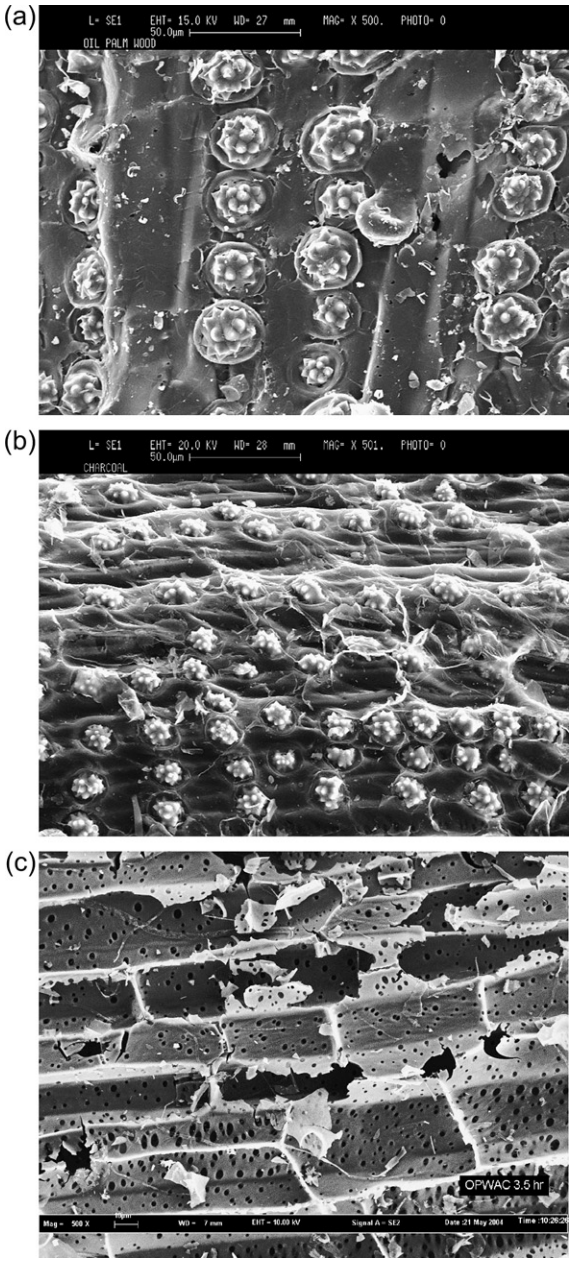

Fig. 7. Magnification of 500× for SEM of (a) oil palm wood, (b) charcoal and (c) activated carbon.

of wood differ significantly from those of charcoal, OPWAC and Norit.

The spectrum for wood displayed the following bands. Significant peak at 3390 cm^{-1}: −OH groups of phenols; 2919 cm^{-1}: two bands for $-CH_2-$ group; 1734 cm^{-1}: C=O stretching vibration of lactones [4]; 1608 cm^{-1} and 1506 cm^{-1}: stretching vibrations of aromatic C=C bonds (i.e. phenyl) [2,34]; 1461 cm^{-1}: aromatic methyl ($-CH_3$) group vibrations [21]; 1425 cm^{-1}: C−O stretch or −OH deformation in carboxylic acids; 1376 cm^{-1}: $-CH_3$ deformation; 1329 cm^{-1}: the syringyl ring with C−O stretching [20]; 1247 cm^{-1}: C−O stretches [35]; 1050 cm^{-1}: ethers −C−O−C− stretches; 897 cm^{-1}: C−H out of plane deformation; 853 cm^{-1}: C−H out of plane bending in benzene derivatives

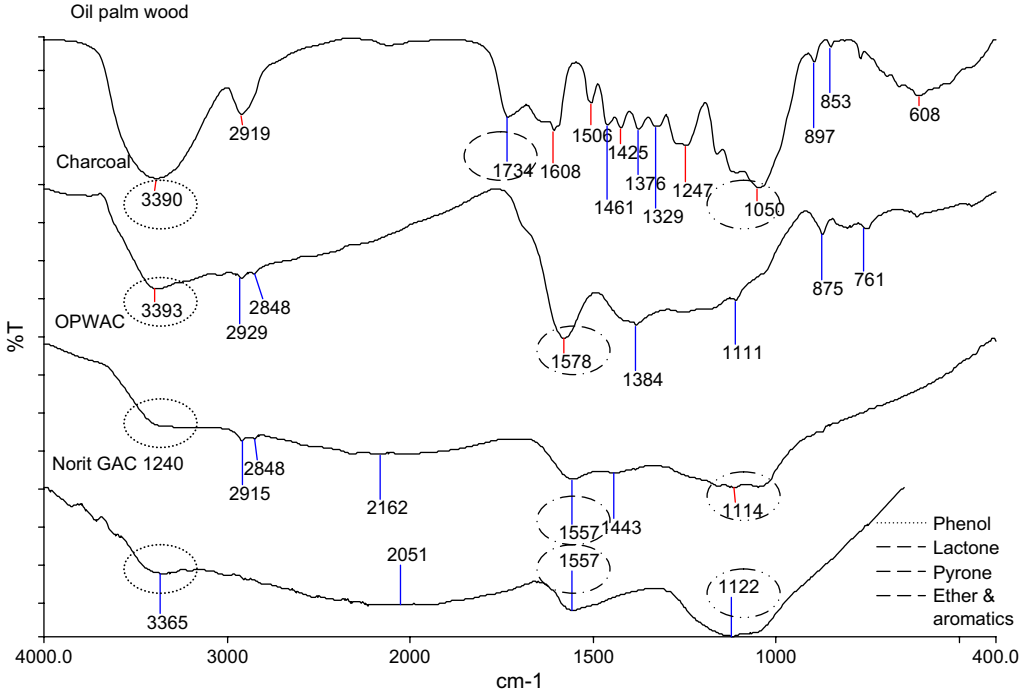

Fig. 8. FTIR diagram of oil palm wood (OPW), oil palm wood charcoal (OPWC), oil palm wood activated carbon (OPWAC) and Norit GAC 1240.

and 608 cm^{-1}: in-plane ring deformation [36]. This spectrum suggests that oil palm wood contains groups such as phenols, lactones, ethers and carboxyl. These results agree with the surface chemistry of other agricultural by-products [37,38].

From the charcoal spectrum, fewer functional groups were detected, indicating that the surface functional groups of oil palm wood experienced chemical changes during pyrolysis. The spectrum displays the following peaks. A peak at 3393 cm^{-1}: −OH group of phenol; 2929 cm^{-1}: methylene group (−CH_2−) with CH stretches; 2848 cm^{-1}: −O−CH_3 or two bands for aldehyde group; 1578 cm^{-1}: C═O stretch of carbonyl group in quinone as well as representing γ-pyrone structure with strong vibrations from a combination of C═O and C═C [4]; 1384 cm^{-1}: −CH_3 deformation; 1111 cm^{-1}: C−H in-plane deformations of the syringyl unit; 875 cm^{-1} and 761 cm^{-1}: C−H out of plane in −CHO aldehydes, pyranose compounds and other benzene derivatives. The pyrolysis process induced the formation of more quinone and pyrone structures. The presence of hydroxyl group of phenolic character causes acidic surface properties whereas carbonyl, quinone and pyranose-like groups bring about surface basicity [34]. Hence, the charcoal surface exhibited both acidic and basic surface functional groups.

The OPWAC spectrum shows the surface functional group with the following peaks. A peak at 2915 cm^{-1}: methylene group (−CH_2−); 2848 cm^{-1}: −O−CH_3 or two bands for aldehyde group; 2162 cm^{-1}: acetals; 1557 cm^{-1}: carbonyl group in quinone as well as γ-pyrone structure; 1443 cm^{-1} and 1114 cm^{-1}: ketones, alcohols, pyrones and aromatic C−H in-plane deformations. The spectra for OPWAC and Norit GAC 1240 (commercial activated carbon) showed great similarity. The formation of stronger peaks for pyrone-type structures, ether and carbonyl groups employed a basic character to both activated carbons [37]. These basic sites in the form of unsaturated bonds between adjacent C-atoms or even non-oxygenated sites with electron donating properties would act as Lewis basic centers that accept protons from aqueous solutions [40].

3.2.5. Methylene blue adsorption

Methylene blue dye (MB), with a molecular size of 19 nm, is a widely used dye in the textile processing industry. MB adsorption serves as a model compound for adsorption of organic contaminants from aqueous solutions [12–14]. Fig. 9 shows the relationship between Langmuir maximum MB adsorption capacity and BET surface area. It was seen that as BET surface area increased, the amount of maximum MB adsorption capacity of OPWAC also increased. Oil palm wood activated carbon subjected to 3.5 h of physical activation (OPWAC3.5)

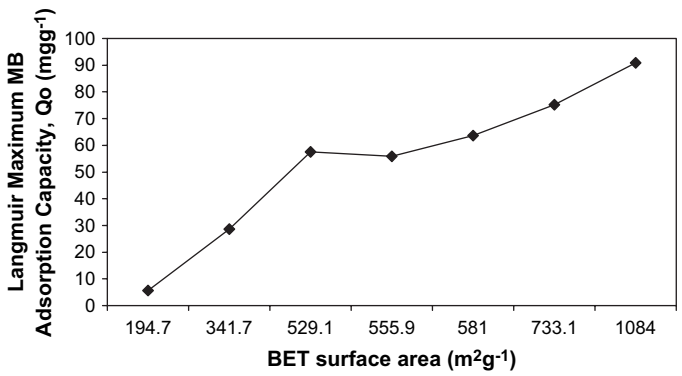

Fig. 9. Relationship between Langmuir maximum MB adsorption capacity and BET surface area.

showed the highest maximum Methylene blue adsorption capacity that is 90.9 mg g^{-1}. This value is 15-fold the adsorption capacity of charcoal.

4. Conclusion

The work prepared relatively well-developed porosity activated carbons via pyrolysis and physical activation using an environmentally friendly pyrolysis pilot plant and an activation pilot plant. The pyrolysis and activation periods affected the final average temperatures, which subsequently influenced the charcoal and activated carbon quantity as well as quality. Under suitable pyrolysis operating conditions of 7 $m^3 h^{-1}$ for 4 h (390 °C) and activation conditions of 7.45 kg limestone fired using airflow rate 202.4 ml s^{-1} for 3.5 h (806 °C), oil palm wood activated carbon of 13.7% yield, 68.3% fixed carbon, 16.9% volatile matters, 4.3% ash, 10.6% moisture, 1084 $m^2 g^{-1}$ BET surface area, 931.6 $m^2 g^{-1}$ micropore surface area and reasonable maximum Methylene blue adsorption capacity of 90.9 mg g^{-1} was obtained. In summary, oil palm wood is an alternative raw material for preparing activated carbon. Most of the activated carbons prepared had a mixture of micro and mesoporosities with high micropore fraction. Hence, they can be utilized for both gas and liquid adsorption applications.

Acknowledgements

The authors gratefully acknowledge the financial support received from Universiti Sains Malaysia through IRPA short-term grant (No. 6035052).

References

[1] Garcia-Garcia A, Gregoria A, Francio C, Pinto F, Boavida D, Gulyurtlu I. Unconverted chars obtained during biomass gasification on a pilot-scale gasifier as a source of activated carbon production. Bioresource Technology 2003;88:27–32.

[2] Lua AC, Guo J. Chars pyrolyzed from oil palm waste for activated carbon preparation. Journal of Environmental Engineering 1999;January: 72–6.

[3] Su W, Zhou L, Zhou YP. Preparation of microporous activated carbon from coconut shells without activating agents. Letters to the Editor. Carbon 2003;41:861–3.

[4] Tsai WT, Chang CY, Wang SY, Chang CF, Chien SF, Sun HF. Preparation of activated carbons from corn cob catalyzed by potassium salts and subsequent gasification with CO_2. Bioresource Technology 2001;78:203–8.

[5] Johns MM, Toles CA, Marshall WE. Activated carbons from low-density agricultural waste. United States patent application 834051; 2003.

[7] Hoi WK, Akmar PF. Solid and liquid fuels. In: Shaari K, Khoo KC, Mohammad Ali AR, editors. Oil palm stem utilisation: review of research, vol. 107. Kuala Lumpur: Forest Research Institute Malaysia; 1991. p. 87–97.

[8] Lim KO, Lim KS. Carbonization of oil palm trunks at moderate temperatures. Bioresource Technology 1992;40:215–9.

[9] Hussein MZ, Zulkarnain Z, Khor KH, Badri M. The preparation of activated carbon from chips of oil palm trunk catalysed by Zn_2Cl_2/CO_2: surface area and porosity studies. Journal of Chemical Technology and Biotechnology 1995;64:35–40.

[10] Wan Daud WMA, Wan Ali WS, Sulaiman MZ. The effects of carbonization temperature on pore development in palm-shell-based activated carbon. Carbon 2000;38:1925–32.

[11] Khalili NR, Pan M, Sandí G. Determination of fractal dimensions of solid carbons from gas and liquid phase adsorption isotherms. Carbon 2000;38(4):573–88.

[12] Banat F, Al-Asheh S, Al-Makhadmeh L. Evaluation of the use of raw and activated date pits as potential adsorbents for dye containing waters. Process Biochemistry 2003;39(2):192–202.

[13] Kannan N, Sundaram MM. Kinetics and mechanism of removal of methylene blue by adsorption on various carbons—a comparative study. Dyes and Pigments 2001;51:25–40.

[14] Kaewprasit C, Hequet E, Abidi N, Gourlot JP. Quality measurements: application of methylene blue adsorption to cotton fiber specific surface area measurement Part 1: methodology. Journal of Cotton Science 1998;2:164–73.

[15] Booth H. Simple technologies for charcoal making. Rome: Food and Agricultural Organization of the United Nations; 1983. p. 1–154.

[16] Byrne CE, Nagle DC. Carbonization of wood for advance materials application. Carbon 1997;35(2):259–66.

[17] Shafizadeh F. Pyrolytic reactions and products of biomass. In: Overend RP, Milne TA, Mudge LK, editors. Fundamentals of thermochemical biomass conversion. London: Elsevier Applied Science Publishers Ltd.; 1985. p. 183–217.

[18] Khalik MS. Studies on the production of charcoal by carbonization using mangrove wood in Malaysia. MSc Thesis, Universiti Sains Malaysia; 2000. p. 1–141.

[19] Ahmad MA. Carbonization of low rank coal. MSc Thesis, Universiti Sains Malaysia; 2002. p. 1–91.

[20] Hoi WK, Low CK, Wong WC. The production of charcoal by the improved transportable metal kiln method. In: Proceeding of Second Asian Conference on Technology for Rural Development, 4–7 December 1985, Kuala Lumpur. p. 1–9.

[21] Elham P, Hamami SM, Jalaludin Zaihan. The carbonization of palm kernel shell by continuous kiln. In: Sixth Asia-Pacific International Symposium on Combustion and Energy Utilization, 20–22 May 2002, Kuala Lumpur. Johor: Universiti Teknologi Malaysia; 2002. p. 308–12.

[22] Simón M, Bonelli PR, Cassanello MC, Cukierman AL. Conversion of wood charcoal waste into activated carbons: effect of the reactive agent. In: Sixth Asia-Pacific International Symposium on Combustion and Energy Utilization, 20–22 May 2002, Kuala Lumpur. Johor: Universiti Teknologi Malaysia; 2002. p. 313–8.

[23] Lua AC, Guo J. Preparation and characterization of activated carbons from oil-palm stones for gas-phase adsorption. Colloids and Surfaces A: Physicochemical and Engineering Aspects 2001;179:151–62.

[24] Rodriguez-Reinoso F, Molina-Sabio M, Gonzalez MT. The use of steam and CO_2 as activating agents in the preparation of activated carbons. Carbon 1995;33(1):15–23.

[25] Minkova V, Razvigorova M, Bjornbom E, Zanzi R, Budinova T, Petrov N. Effect of water vapour and biomas nature on the yield and quality of the pyrolysis products from biomass. Fuel Processing Technology 2001;70:53–61.

[26] Cagnon B, Py X, Guillot A, Stoeckli F. The effect of carbonization/activation procedure on the microporous texture of the subsequent chars and active carbons. Microporous and Mesoporous Materials; 2003; 273–82.

[27] Raveendran K, Ganes A, Khilart KC. Influence of mineral matter on biomass pyrolysis characteristics. Fuel 1995;74(12):1812–22.

[28] Rockcarb. Manufacturer of Industrial Adsorbents. Available from: www.rockcarb.com/html/specification.htm; 2004 [accessed 30.06.04].

[29] Cao N, Darmstadt H, Soutric F, Roy. Thermogravimetric study on the steam activation of charcoals obtained by vacuum and atmospheric pyrolysis of softwood bark residues. Carbon 2002;40:471–9.

[30] Linares-Solano A, Martin-Gullon I, Salinas-Martinez de Lecea C, Serranp-Talavera B. Activated carbons from bituminous coal: effect of mineral matter content. Fuel 2000;79:635–43.

[31] Lua AC, Yang T. Properties of pistachio-nut-shell activated carbons subjected to vacuum pyrolysis conditions. Letters to the Editor. Carbon 2004;42:219–38.
[32] Wan Daud WMA, Wan Ali WS, Sulaiman MZ. Effect of activation temperature on pore development in activated carbon produced from palm shell. Journal of Chemical Technology and Biotechnology 2002; 78:1–5.
[33] Khoo KC, Killmann W, Lim SC, Halimahton M. Characteristics of the oil palm stem. In: Shaari K, Khoo KC, Mohammad Ali AR, editors. Oil palm stem utilisation: review of research, 107. Kuala Lumpur: Forest Research Institute Malaysia; 1991. p. 15–28.
[34] Boehm HP. Surface oxides on carbon and their analysis: a critical assessment. Carbon 2002;40:145–9.
[35] Guo J, Lua AC. Textural and chemical characterization of activated carbon prepared from oil palm stone with H_2SO_4 and KOH impregnation. Microporous and Mesoporous Materials 1999;32:111–7.
[36] University Potsdam. IR-Wizard. Available from: http://www.chem.uni-potsdam.de/cgi-bin/irwiz2.pl; 2004 [accessed 12.05.04].
[37] Sun RC, Tomkinson J. Fractional separation and physico-chemical analysis of lignins from the black liquor of oil palm trunk fibre pulping. Separation Purification Technology 2001;24:529–39.
[38] Al-Degs Y, Khraisheh MAM, Alle SJ, Ahmad MN. Effect of carbon surface chemistry on the removal of reactive dyes from textile effluent. Water Research 2000;34(3):927–35.
[40] Moreno-Castilla C. Adsorption of organic molecules from aqueous solutions on carbon materials. Carbon 2000;42:83–94.